IEEE Access
Multidisciplinary | Rapid Review | Open Access Journal

Received December 29, 2019, accepted January 4, 2020, date of publication January 9, 2020, date of current version January 16, 2020.

Digital Object Identifier 10.1109/ACCESS.2020.2965285

Remaining Useful Life Assessment of Slewing Bearing Based on Spatial-Temporal Sequence

WEIGANG BAO, XIAODONG MIAO, HUA WANG, GUICHAO YANG, AND HAO ZHANG
School of Mechanical and Power Engineering, Nanjing Tech University, Nanjing 211816, China

Corresponding author: Xiaodong Miao (mxiaodong@njtech.edu.cn)

This work was supported in part by the National Natural Science Foundation of China under Grant 51875273 and Grant 61906088, and in part by the Project of Jiangsu Provincial Six Talent Peaks under Grant GDZB-033.

ABSTRACT Slewing bearing is one of key components in the large size machinery and its remaining useful life (RUL) prediction is required to schedule a future action to avoid catastrophic events, extend life cycles, etc. The vibration-based method has been widely used in the RUL prediction. However, the spurious fluctuation usually exists in the vibration signal when the machines are operated under complex conditions. In order to enhance performance of RUL prediction model, two kinds of new health indicators are constructed by the spatial-temporal (ST) information firstly. One is the temporal indicators, which are derived by using the smoothing mean values of positive and negative vibration signal. Another is the spatial indicator, which is defined by fusing the multi-features extracted from the balance position information of vibration signal. During this process, a new data processing method proposed in this paper improves the quality of the vibration data and increases the number of samples. And then, the RUL prediction model is presented by combing the ST indicators and long-short-term memory network (LSTM) to establish the relationship between the ST indicators and the RUL of slewing bearings and overcome the sparsity of data. Moreover, in order to accelerate the adjustment of ST-LSTM model, a fine-tuning ST-LSTM model is further proposed by incorporating the generative adversarial networks (GAN) into the ST-LSTM. Experimental results verify that the proposed RUL prediction model can well estimate the RUL of slewing bearings and its performance is superior to some existing methods.

INDEX TERMS Balanced position, GAN, life prediction, slewing bearing, spurious fluctuation, ST-LSTM.

I. INTRODUCTION

Slewing bearings are widely used in mechanical equipment and called the joints of machine. Due to the larger size of the slewing bearing, any unexpected failure of bearings may cause more serious problems than failure of the small bearing. Minor failure may cause a drop in productivity or downtime of mechanical equipment and serious failures can cause major safety problems [1]–[4]. To ensure safety and reliability of the slewing bearing, preventive and corrective maintenance are necessary. The effective assessment of RUL can avoid unnecessary spending time and consumption in maintenance [5]–[7]. Condition monitoring and life prediction provide the maintenance of slewing bearing with an important basis [8]–[11]. The life prediction of the slewing bearing is mainly composed of two parts. One is the signal processing, the other is the establishment of life prediction model [12].

In signal processing, some important characteristics including the correlation, monotonicity and robustness were combined to select features, which made the life model more effective and efficient [13]. A spectral correlation density combination method was put forward to determine the fault frequency and get better fault recognition [14]. The premise of these methods for processing data requires high quality signal data which are often obtained in a quiet laboratory. The vibration signal collected in-situ environment will be interfered by various noises. The linear rectification technique (LRT) was proposed to handle spurious fluctuation which are not caused by faults [15], [16]. RMS Entropy Estimator (RMSEE) was applied to avoid these fluctuations, which improve the quality of the prognostic approach [17]. The methods with feature extraction and selection are benefit to the establishment of the model and the corrections of fluctuations are very effective for spurious fluctuations in the

The associate editor coordinating the review of this manuscript and approving it for publication was Yingxiang Liu.

vibration signal. However, under actual working conditions, spurious fluctuations and fluctuations caused by fault signals might co-exist. Currently, there is no the technique to judge whether this fluctuations are spurious fluctuations or not in these literature. Fluctuations are not necessarily invalid feature and some valuable fluctuations need to be retained. If all features are repaired as spurious fluctuations, some valuable fault information will be lost, and the state assessment of the slewing bearing may not be accurate. In this case, balance position of slewing bearing is extracted in the paper. The information of the balance position of the slewing bearing can well reflect the current working condition of operation. Balance position is usually kept constant under normal operating conditions, but when a fault occurs, the fluctuation will occur in balance position due to the sudden impact. In the actual working environment, the collected vibration signal of slewing bearing often has large fluctuation. This fluctuation is mainly caused by faults and external disturbances. The spurious fluctuations generated by external disturbances can mask the fluctuations caused by the faults or be mistaken for the fluctuations caused by the faults. Spurious fluctuation may seriously interfere with the evaluation of RUL of the slewing bearing. This is one of the important reasons why many fault diagnosis techniques have low accuracy in practical work. Hence, the high quality data is the foundation of health assessment. However, under complicated working conditions, the collected vibration data are interfered by various factors so the spurious fluctuations are abnormally frequent. Fortunately, the defined balance position is a good indicator for discriminating spurious fluctuations.

In the slewing life prediction model, the artificial intelligence methods are applied more and more widely [18], [19]. Some features were fused into health indicators by recurrent neural network (RNN) to characterize the operational status of the bearing and the assessment of health status was realized by the combination of multiple physical signals and artificial neural network (ANN) [20], [21]. Zhu, et al. constructed a life prediction model of multi-scale convolutional neural network (MSCNN), which kept the global and local information synchronously [22]. The long-short-term memory network (LSTM) was used to predict remaining useful life (RUL) of rolling element bearing and applied to the prediction of fault time series, which achieved good prediction result [23], [24]. Long short-term memory recurrent neural network (LSTM-RNN) was employed to the prediction field, improving the accuracy of the model. However, existing prediction models only consider time series. Also, the data of slewing bearing generally has the characteristic of sparsity, so the life prediction model built on the slewing bearing will deviate from the actual model. In this paper, ST-LSTM is proposed to solve this problem, greatly improving the accuracy of the prediction model. Then, the generative adversarial networks ST-LSTM (GAN-ST-LSTM) model is constructed to fine-tune the ST-LSTM model to make this model more excellent.

The main contributions of this paper are:

(1) It is the first time to use the spatial information of the slewing bearing. The extracted spatial information has actual information value, which represents the strength of the fault in slewing bearing.

(2) The proposed method can obtain high quality data of vibration signal. The spatial information is used to determine whether the random fluctuation in the vibration signal belongs to the fault signal or not. The untrue fault signal can be regarded as defect data and then the higher quality data can be obtained through the repairing process.

(3) Three effective and reliable sample data can be extracted from one vibration signal, which overcomes the problem of insufficient training samples.

(4) The accuracy of the prediction model is greatly improved. ST-LSTM proposed in this paper makes the life prediction model of slewing bearing have spatial-temporal characteristic. In ST-LSTM, a close relationship is stablished between spatial-temporal indicators and RUL of slewing bearings. On the basis of ST-LSTM, the GAN-ST-LSTM is further constructed to enhance the ability of adaptive adjustment of the life prediction model and makes the life prediction model of ST-LSTM more accurate.

The remainder of this paper is organized as follows. In Section II, the method of how to achieve spatial and temporal indicators of slewing bearing is introduced in detail. In Sections III, the principle of LSTM is briefly described. Then, according to spatial and temporal indicators obtained, the structure of the ST-LSTM proposed in this paper is specifically described. Finally, an optimization model GAN-ST-LSTM is constructed. In Section VI, the slewing bearing test-rig used to collect vibration signals and analysis of experimental results with some methods are presented. The conclusions are drawn in Sections V.

II. SPATIAL AND TEMPORAL INDICATORS

Spatial and temporal indicators are important indicators for the health status of slewing bearing and the key to building ST-LSTM. The flow chart of how to achieve spatial-temporal indicator is shown in Fig. 1.

A. ACQUISITION OF SPATIAL-TEMPORAL INFORMATION

The slewing bearing is an important rotating component in the mechanical device. Its spatial information is generally ignored by scholars. The main reason is that the slewing bearing is generally considered to have a fixed spatial position during operation. However, when a part of the slewing bearing fails, unbalanced forces are generated. The unbalanced forces will produce strong fluctuations which can change the balance position of the slewing bearing in a short time. Therefore, the balance position of the slewing bearing can well reflect the failure of the slewing bearing and it is a non-negligible indicator. The balance position of the slewing bearing reflects its spatial information. As far as we know, the spatial information of slewing bearing is difficult to capture

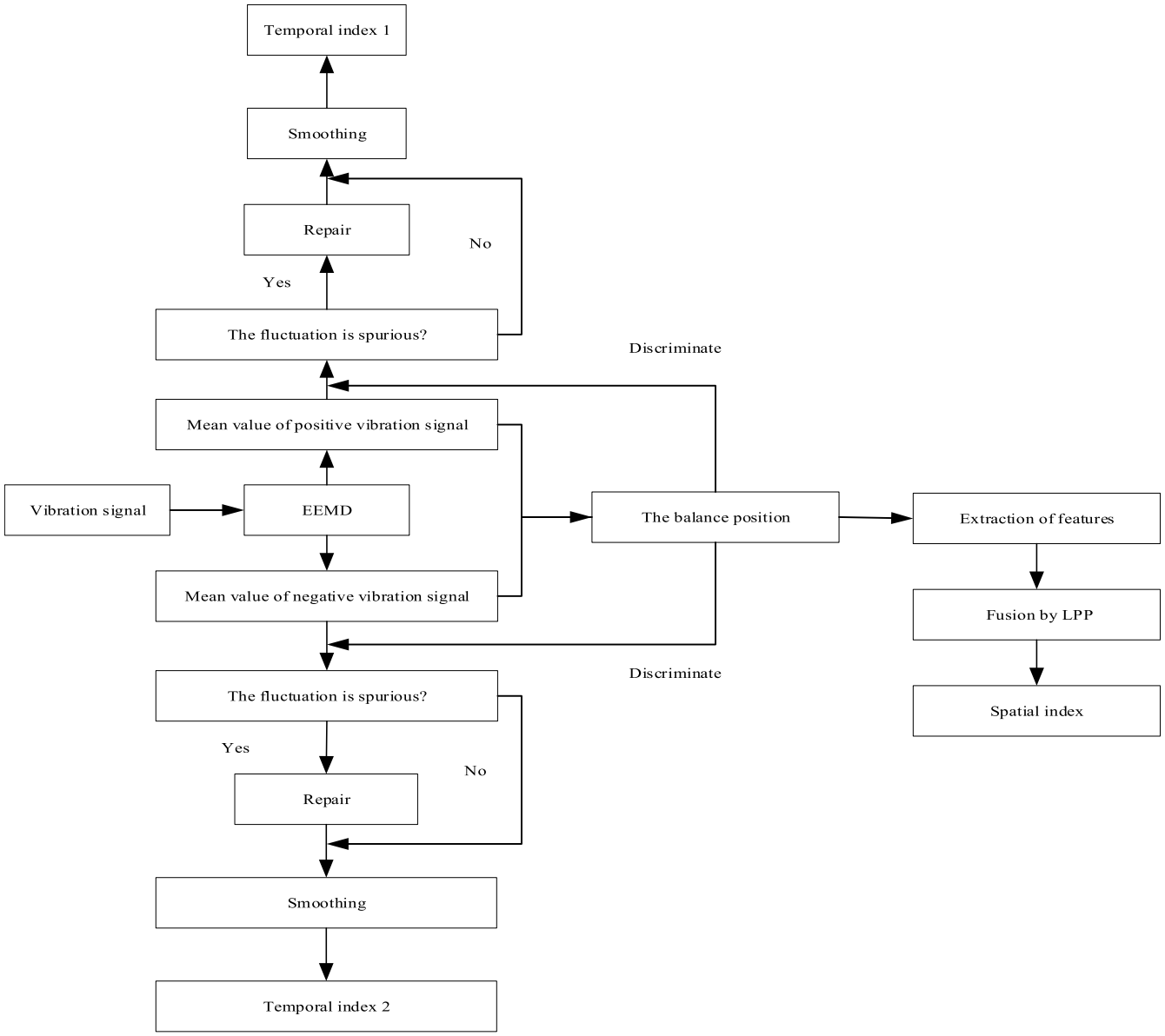

FIGURE 1. The flow chart of spatial-temporal indicator.

and no one has tried to extract this indicator. There are often the large spurious fluctuations in the vibration signal, which will interfere with the life prediction model of slewing bearing. To solve this problem, the spatial information extracted from vibration signal is used to identify spurious fluctuations. The method of extracting this spatial information is constructed as follows. Two extraction methods are selected in this paper to determine which way is more suitable for extracting spatial information.

Require: $P \leftarrow$ the sum of all positive values in the vibration signal in one second; $n1 \leftarrow$ the number of positive values of the vibration signal in one second; $N \leftarrow$ the sum of all negative values in the vibration signal in one second; $n2 \leftarrow$ the number of negative values of the vibration signal in one second; $S \leftarrow$ balance position; $M_p \leftarrow$ positive mean value; $M_n \leftarrow$ negative mean value.

Detailed steps are as follows:

Step I: Select a vibration signal of 4500 seconds during the full-life vibration period. The data of every second is a separately selected individual.

Step II: Calculate M_p and R_p of the positive vibration signal in each second.

$$M_p = \frac{P}{n1}$$
$$R_p = \sqrt{\frac{\sum_{i}^{n1} x_i \wedge 2}{n1}} \quad (1)$$

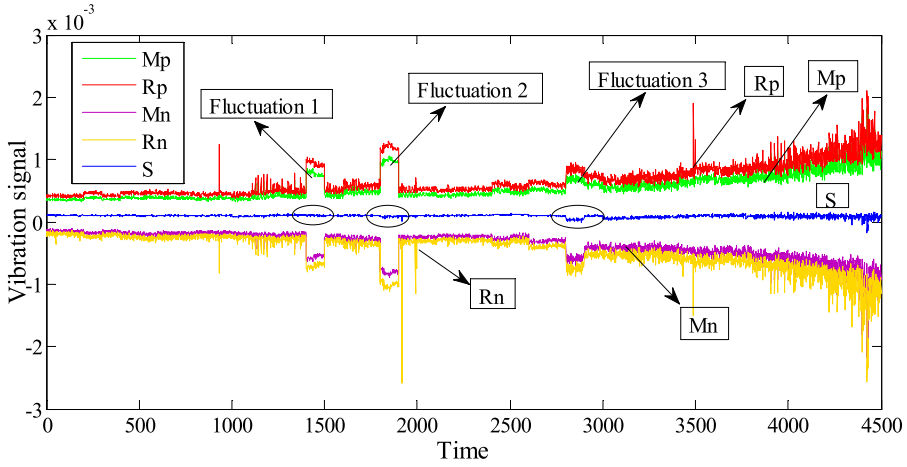

FIGURE 2. Extraction of spatial-temporal information.

Step III: Calculate the M_n and R_n of the negative vibration signal in each second.

$$M_n = \frac{N}{n2}$$
$$R_n = \sqrt{\frac{\sum_{i}^{n2} x_i\text{^}2}{n2}} \tag{2}$$

Step IV: Calculate S.

$$S = \frac{M_p + M_n}{2} \tag{3}$$

The acceleration sensor is used to collect the vibration signal and the sampling frequency is 2048. x_i represents the ith data in one second. Acquired vibration signal is denoised by EEMD. Then vibration signal obtained after extraction are shown in Fig. 2 below. One point on the abscissa is equal to 4 minutes.

It can be seen from the Fig. 2 that R_p and R_n are greatly affected by abnormal noise value, resulting in instability during the life cycle. M_p and M_n are relatively stable and the data is reliable. If R_p and R_n are used to calculate S, abnormal noise signals in S will be relatively amplified. Thus, the M_p and M_n are more suitable for calculating S.

Specific reasons of extracting spatial indicator by this method:

(1) Compared with the random selection of vibration signals, the value obtained by the mean method of separating positive and negative signals is more representative, which greatly eliminates the occasional interference.

(2) The difference of the vibration signal reflects the difference of the position information, so the balance position change can be extracted from the vibration signal. When the slewing bearing fails, the vibration signal becomes complicated and instantaneous impact forces cause the changes in the balance position.

(3) Random fluctuations caused by external noise signals that may exist in M_p and M_n can be offset each other. The sensor and the slewing bearing are fastened together despite the interference of external noise signals. The balance position of the slewing bearing has not changed with respect to the position of sensor. The influence of the noise signal on the positive and negative values of the vibration signal is almost the same in a short time. So S can exclude spurious fluctuations caused by external noise. S should be constant at different times under normal conditions, however, the slight changes often occur due to manufacturing errors and installation errors and work failures. S is a good spatial information reflecting the health status of the slewing bearing. According to information of S, it can be judged whether random fluctuation caused by faults or not.

As shown in Fig. 2, taking M_p as an example, although M_p has abnormal fluctuation in area of fluctuation 1 and fluctuation 2 respectively, their corresponding S has no significant change. On the contrary, the corresponding S of M_p in fluctuation 3 has undergone a significant step change, explaining that a fault has occurred within the time corresponding to the fluctuation 3. The flutuations in area of fluctuation 1 and fluctuation 2 are not caused by faults, which is unfavorable for the life prediction of slewing bearing. Valuable fault information is included in fluctuation 3. If it is considered as spurious fluctuation information to repair, the life assessment of the slewing bearing will be deviated from real life. This area of fluctuation 3 needs to retain the original information. M_n and M_p have the same analysis process. Nonlinear rectification technique is used to handle spurious fluctuations in fluctuation 1 and fluctuation 2 to get new data and the results are shown in the Fig. 3.

After processing by nonlinear rectification technique, the repaired vibration signal is illustrated in Fig. 3. It is worth noting that we have obtained three data sets now while there was only one training set for raw vibration signal. Moreover, by removing random fluctuations in raw vibration signal, the training samples contain higher quality data. The high quality data and increasing number of training samples provide a more reliable basis for the RUL assessment of

TABLE 1. The information of features.

Feature	Expression	Feature	Expression
Maximum	$X_{\max} = \max\{\lvert x_n \rvert\}$	Kurtosis	$\beta_n = \frac{1}{n}\sum_{n=1}^{n} x_n^4$
Root amplitude	$X_{n(r)} = \left[\frac{1}{n}\sum_{n=1}^{n}\sqrt{\lvert x_n \rvert}\right]^2$	Waveform indicators	$S_{n(f)} = \frac{X_{n(rms)}}{\lvert \bar{X}_n \rvert}$
Variance	$\sigma_n^2 = \frac{1}{n}\sum_{n=1}^{n}(x_n - \bar{X}_n)^2$	Peak index	$K_v = \frac{\beta}{X_{n(rms)}^4}$
Root mean square	$X_{n(rms)} = \sqrt{\frac{1}{n}\sum_{n=1}^{n} x_n^2}$	Pulse indicator	$S_{n(f)} = \frac{X_{n(rms)}}{\lvert \bar{X}_n \rvert}$
Absolute mean	$\lvert \bar{X} \rvert = \frac{1}{N}\sum_{n=1}^{N}\lvert x_n \rvert$	Amplitude margin	$CL_{n(f)} = \frac{X_{n(\max)}}{X_{n(r)}}$
Mean square frequency	$Msf = \frac{\sum_{i=1}^{n} f_i^2 p_i}{\sum_{i=1}^{n} p_i}$	Center of gravity frequency	$Fc = \frac{\sum_{i=1}^{n} f_i p_i}{\sum_{i=1}^{n} p_i}$
IMF energy	$X_{\text{imf}} = \sum_{i=1}^{n}\lvert C_i(t) \rvert^2$	Frequency standard deviation	$VF = \frac{\sum_{i=1}^{n}(f_i - Fc)^2 p_i}{\sum_{i=1}^{n} p_i}$

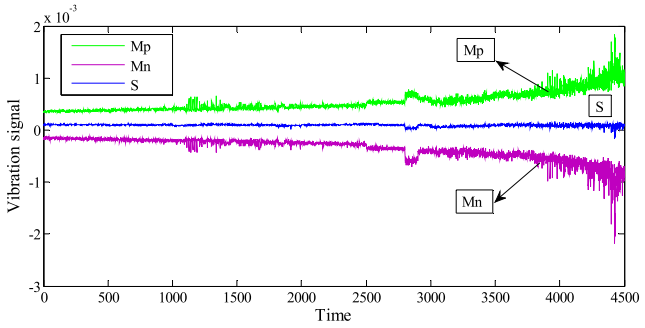

FIGURE 3. The repaired spatial-temporal information.

slewing bearing subsequently. Since the data contained in S are not obvious, further processing is required to extract obvious features.

B. TEMPORAL INDICATOR

In order to get the more accurate temporal indicators, a smooth curve method is performed on M_p and M_n. The results are shown in Fig. 4.

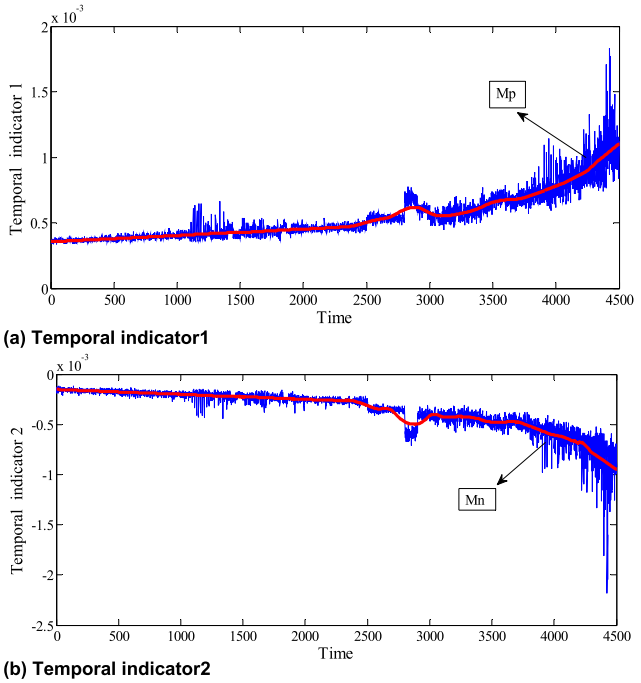

FIGURE 4. Temporal indicator.

C. SPATIAL INDICATOR

Although a lot of fault information can be reflected by S to some extent, the information in S is relatively weak. Hence, some classical features are used to represent the fault information in S as reported in Table 1.

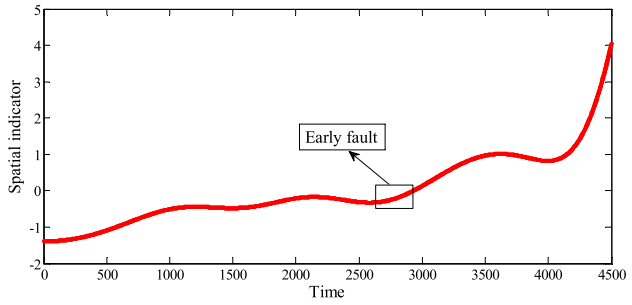

FIGURE 5. Spatial indicator.

x_n is the nth point of the S, f_i is the frequency and p_i is power spectrum amplitude. *Ci(t) is* intrinsic mode functions.

After the above features are extracted, the fusion process is performed on them by using locality preserving projections (LPP) [25]–[27]. The neighborhood structure of the data can be preserved optimally by LPP which is suitable to fuse the features of S. The fusion result of outstanding features is regarded as the spatial indicator, as shown in Fig. 5.

In Fig. 5, the moment of the early fault is at the point of producing the significant fluctuations in S. Overall, the extracted spatial indicator can reasonably reflect the degradation trend of the slewing bearing. Early failures are critical to the life assessment of slewing bearing. Slewing bearing is in a serious degradation stage after 4000 point.

III. LIFE PREDICTION MODEL OF SLEWING BEARING

A. LSTM

As an improved model of the traditional RNN model, LSTM has better ability to learn long-term memory information than traditional RNN models. Also, in the field of natural language processing and image recognition, LSTM has a bigger advantage than RNN [28]. The cell unit and three gates are included in the core structure of LSTM. The three gates are input gate, forget gate and output gate. The input of new information is controlled by the input gate. The amount of information discarded is determined by the forget gate and the output of the final output information is filtered by the output gate. Cell unit determines the state of the cell at the current time [29]. The structure of LSTM is shown in the Fig. 6.

B. ST-LSTM

Usually, a large amount of data need to be trained and learned to ensure the functional integrity of these gates in LSTM. In the field of deep learning, the lack of sufficient sample data is a tricky problem which adversely affects the accuracy of the life prediction of slewing bearings. Fortunately, through the data processing earlier in this paper, we can get three sets of valid data from vibration signals. The sparsity of the data may lead to the deviation between the life prediction model and the real model. Establishing a connection between training samples can solve this problem. The relationship among spatial and temporal indicator and the RUL of the slewing bearing is interrelated and inseparable. This relationship can be used as an implicit information to guide the learning of the gates in LSTM, which plays a role in enhancing training samples. The relationship between them is shown in Fig. 7.

As demonstrated in Fig. 6, LSTM can't combine the temporal indicator and the spatial indicator effectively. Also, it is not enough to establish a precise life prediction model of the slewing bearing by consider only the temporal indicator. It is necessary to combine temporal indicators, spatial indicators and RUL. The established life prediction model of the slewing bearing should have the spatial-temporal characteristics. In order to solve these problems, as show in Fig. 8, ST-LSTM is proposed in this paper. ST-LSTM can effectively combine spatial and temporal indicator of slewing bearing under working condition.

The prediction of RUL model is constructed as follows:

Require: i_t ← the input gate; f_t ← the forget gate; o_t ← the output gate; c_t ← the state of cell; h_t ← the final output; b ← the bias of each gate; σ ← the sigmoid function in each state; w ← the weights matrix. The subscripts of the weight matrix have their own meanings. For example, w_{xi} represents the weight matrix of hidden state to input gate; w_{xo} represents the weight matrix of input gate

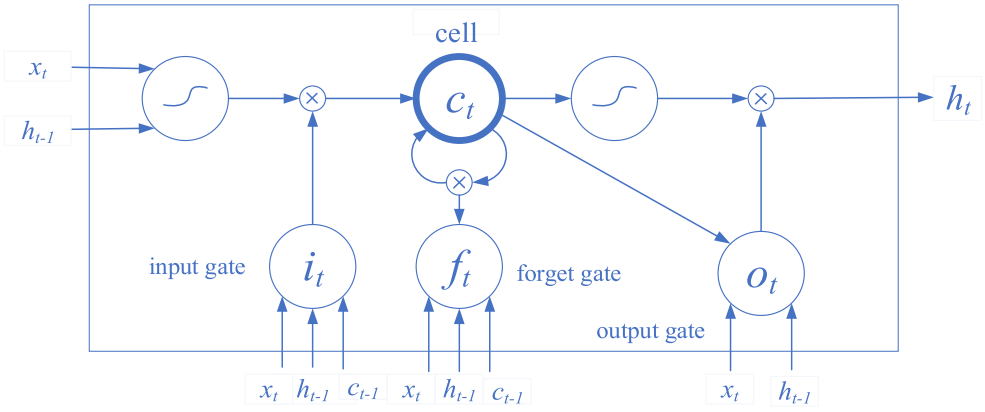

FIGURE 6. The structure of LSTM.

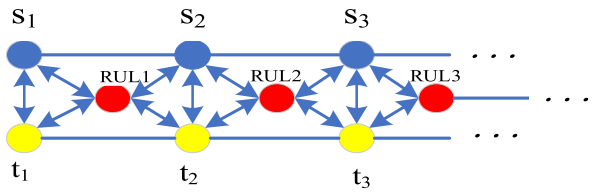

FIGURE 7. The spatial-temporal connection of RUL.

to output gate; w_{cf} represents the weight matrix of cell to forget gate. s_t ← the spatial indicator expression of slewing bearing in the continuous time interval between t- 1 time and t time; t_t ← the temporal indicator expression of slewing bearing in the continuous time interval between t - 1 time and t time; cf ← correction factor; $w_{t(st)}$ ← weight of temporal difference; $w_{s(st)}$ ← weight of spatial difference.

The main steps of ST-LSTM:

Step I: Calculate the s_t and t_t sequences according to the obtained spatial and temporal indicator of slewing bearing. Construct ST gate with the s_t and t_t with (6).

$$\begin{aligned} s_t &= (\text{spatial indicator})_t - (\text{spatial indicator})_{t-1} \\ t_t &= (\text{temporal indicator})_t - (\text{temporal indicator})_{t-1} \end{aligned}$$

Step II: The life prediction model of the slewing bearing is obtained according to the ST-LSTM model. The final output state h_t is the result of the ST-LSTM, h_t represents the RUL of the slewing bearing by ST-LSTM at the moment.

Fine tune model of ST-LSTM (GAN-ST-LSTM):

Step III: ST-CNN is used to discriminate the life prediction model of slewing bearing. If ST -CNN discriminates that the model produced by ST-LSTM is false, the penalty factor will also be brought in and ST-LSTM will regenerate the model until ST-CNN cannot discriminate between the generated model and the real model. Otherwise, ST-LSTM will carry out the life prediction of next stage.

Step IV: Repeat step III until the prediction of life cycle is completed. h_t represents the RUL of the slewing bearing by GAN-ST-LSTM.

The principle of ST-LSTM is given as follows:

Input gate: The input gate consists of the hidden state of the previous moment and the existing sequence. New information will be selectively recorded into the cell state. Some valuable information will be stored in the cell state. Its calculation formula is

$$i_t = \sigma_i \left(w_{xi} x_t + w_{hi} h_{t-1} + w_{ci} \odot c_{t-1} + b_i \right) \tag{4}$$

Forget gate: In forget gate, the sigmoid activation function is used to control the output between 0 and 1. 0 means forgetting all the information and 1 means keeping all information. The forget gate will selectively forget the information in the hidden state of the previous moment sequence. These forgotten messages are generally unimportant or highly disruptive, such as some noise information in the vibration signal. Its calculation formula is

$$f_t = \sigma_f \left(w_{xf} x_t + w_{hf} h_{t-1} + w_{cf} \odot c_{t-1} + b_f \right) \tag{5}$$

Spatial-temporal gate: In order to combine the spatial indicator and the temporal indicator, the model of life prediction of slewing bearings needs to have spatial-temporal characteristics. ST gate is added to the LSTM model. The input of the ST gate is composed of three part, besides the input x_t, t_t and s_t are added. The information of t_t and s_t exists as a separate gate, showing the temporal and spatial correlation more directly. On the one hand, st_t participates in the state of the currently input unit, which can control the temporal and spatial information of t_t and s_t into a new cell state. On the other hand, 1-st_t participates in the cell state of the previous moment, which can filters out unimportant historical information and interference signals together with the forgetting gate. In the structure of this ST-LSTM, st_t can be regarded as the input gate of the spatial-temporal characteristics and 1-st_t

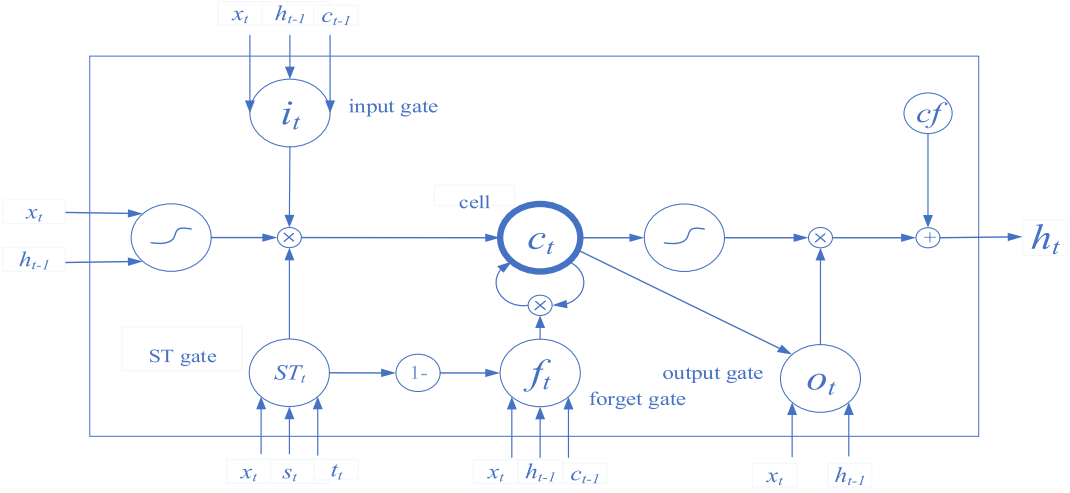

FIGURE 8. The structure of ST-LSTM.

can be regarded as the forget gate of the spatial-temporal characteristics. They can control the spatial-temporal information together so the model has spatial-temporal characteristics. In this way, the relationship between the spatial indicator and the temporal indicator in the slewing life prediction model can be fully studied. The calculation formula of ST-gate is as follows:

$$st_t = \sigma_{st}\left(w_{x(st)}x_t + w_{t(st)}t_t + w_{s(st)}s_t + b_{st}\right) \tag{6}$$

Cell: The improved cell can better integrate important historical information and existing information, so the current cell state stores the comprehensive information of each gate and the result of cell is the candidate value. In the ST-LSTM network layer, spatial-temporal information st_t will participate in the current cell state and 1-st_t will be added to the cell state at the previous moment. The calculation formula of cell in LSTM is

$$c_t = f_t \odot c_{t-1} + i_t \odot \tanh\left(w_{xc}x_t + w_{hc}h_{t-1} + b_c\right)$$

Its improved calculation formula in ST-LSTM is

$$c_t = f_t \odot c_{t-1} \odot (1 - st_t) + i_t \odot \tanh\left(w_{xc}x_t + w_{hc}h_{t-1} + b_c\right) \odot st_t \tag{7}$$

Output gate: The role of the output gate is to control the amount of information, which is transferred from current cell state to output value h_t. The judgment information will be saved in the hidden layer. The function of the activation function tanh is to keep the output value of the cell at the current time in the interval $[-1, 1]$. In order to increase the accuracy of the model, the correction factor cf is added to the ST-LSTM model and the correction factor represents the direction of actual output life. The correction factor can correct the output result.

The calculation formula of output gate in ST- LSTM is as:

$$o_t = \sigma_o\left(w_{xo}x_t + w_{ho}h_{t-1} + w_{co} \odot c_t + b_o\right) \tag{8}$$

The calculation formula of final output in LSTM is

$$h_t = o_t \odot \tanh(c_t + b)$$

Its improved calculation formula in ST-LSTM is

$$h_t = o_t \odot \tanh(c_t + b) + cf \tag{9}$$

C. GAN-ST-LSTM

Generative Adversarial Network (GAN) has two networks, one is generator and the other is discriminator. Generator is guided by discriminator to train model. Discriminator is used to discriminate the generated model. GAN is widely used in many areas of artificial intelligence [30], [31]. For example, in the field of image denoising [32] and image generation [33], [34], GAN has achieved good results. In this paper, GAN-ST-LSTM is proposed to fine tune the prediction model of slewing bearing. It is a secondary optimization of LSTM. In the model of GAN-ST-LSTM, ST-LSTM is considered as generator, ST-CNN is considered as discriminator. The goal

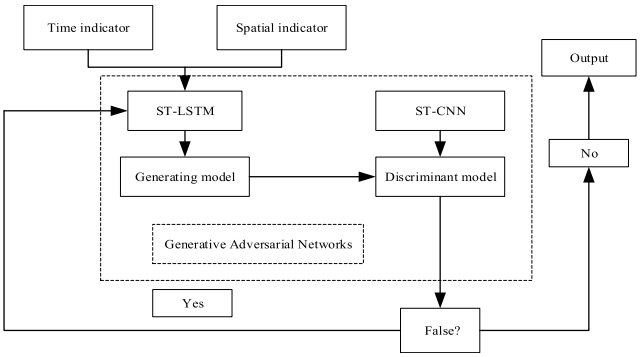

FIGURE 9. The structure of GAN-ST-LSTM.

of the discriminant model ST-CNN is to discriminate whether the model generated by the ST-LSTM is false. If the discriminant result cannot distinguish between LSTM model and the real model, the result of ST-LSTM is RUL of slewing bearing. Otherwise, ST-LSTM will regenerate the model until ST-CNN cannot discriminate between the generated model and the real model. The structure of GAN-ST-LSTM is shown in Fig. 9.

In order to distinguish between real access sequences and access sequences generated by the generator. Spatial-temporal information is introduced into the convolutional neural network (CNN) to enhance discriminative ability [28]. The principle of ST-CNN is as follows:

Give a RUL sequence,

$$x = \{R_1, R_2, R_3, \cdots R_N\} \tag{10}$$

and convert it to an access node with spatial-temporal information

$$R_i^{st} = R_i \oplus s_i \oplus q_i \tag{11}$$

$\oplus$ is splicing operation and the access sequence with spatial-temporal information can be obtained.

$$x^{st} = \{R_1^{st}, R_2^{st}, R_3^{st} \cdots R_N^{st}\} \tag{12}$$

Express it as a matrix:

$$\zeta_{1:N} = R_1^{st} \oplus R_2^{st} \oplus R_3^{st} \oplus \cdots \oplus R_N^{st} \tag{13}$$

Extract features of the matrix using multiple filters $\{f_1, f_2, f_3, \cdots f_m\}$. The size of filter's window is a_j, The convolution of $\zeta_{1:N}$ is as follows:

$$e_i^j = \sigma\left(f \otimes \zeta_{i:i+aj-1} + b\right) \quad i = 1, 2, \cdots N - a_j + 1 \tag{14}$$

$\otimes$ is a bitwise multiply summation operation, and b is a bias term. The corresponding feature map of f_j is

$$F_j = \{e_1^j, e_2^j, \cdots, e_{N-a_j+1}^j\} \tag{15}$$

Filters with different window size can extract different sequence features. For the resulting feature map $\{F_1, F_2, \cdots, F_M\}$, perform the max-pooling over time.

$$\widetilde{e_j} = \max\{e_1^j, e_2^j, \cdots, e_{N-a_j+1}^j\} \tag{16}$$

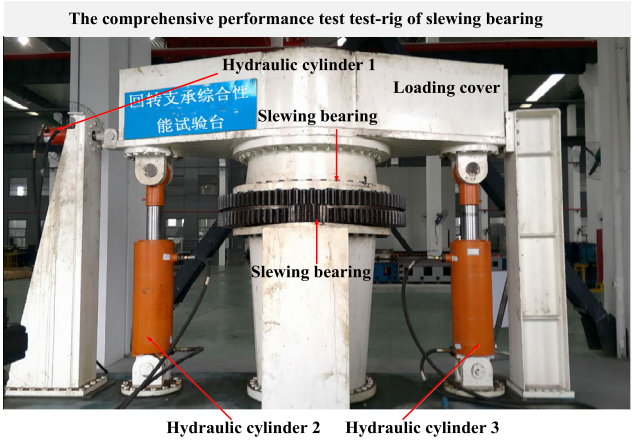

FIGURE 10. The structure of slewing bearing test-rig.

TABLE 2. Main parameters of slewing bearing.

The raceway diameter(mm)	730	Inner ring diameter(mm)	621.6
Outer ring diameter(mm)	811	Ball diameter(mm)	22.525
The number of bolt	36	The number of balls	91
Contact angle	45°	raceway surface hardness(HRC)	57
Inner and outer ring materials	42Cr Mo	Ball material	GCr15
Preload(KN)	83	rotating speed(rpm)	4

Get M-dimensional feature vector.

$$F = \underset{1}{\tilde{e}} \oplus \underset{2}{\tilde{e}} \oplus \cdots \oplus \underset{M}{\tilde{e}} \tag{17}$$

Enter the feature vector into the following classifier to get the probability that this sequence is a real access sequence.

$$\hat{y} = \sigma\left(w_o * F + b_o\right) \tag{18}$$

IV. EXPERIMENT AND RESULTS

A. EXPERIMENT OF SLEWING BEARING

The comprehensive performance test-rig of slewing bearing is mainly composed of mechanical system, hydraulic system, measurement and control system. The function of the hydraulic cylinder's combination loading is to simulate the force of the actual working environment. As is shown in Fig. 10, hydraulic cylinder 1 provides axial force. The combination of hydraulic cylinder 2 and hydraulic cylinder 3 can provide radial force and overturning moment. The pinion on the outer ring of the slewing bearing is driven by the hydraulic motor to realize the rotation of the slewing bearing. The collection of sensing data and the control of hydraulic system are realized by measurement and control system. The real-time vibration signal of the slewing bearing is saved by the measurement and control system. The National Instruments (NI) data acquisition card is included in the measurement and control system to complete data collection. The main parameters of slewing bearing are shown in Table 2. In the measurement

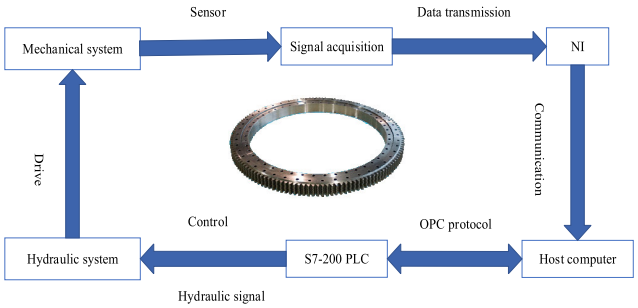

FIGURE 11. The flow chart of the test-rig.

FIGURE 12. The disassembly of the slewing bearing.

and control system, the host computer communicates with the Siemens Programmable Logic Controller (PLC) through the Object Linking and Embedding for Process Control (OPC) protocol. PLC issued commands to control the operation of different hydraulic cylinders and hydraulic motors. The flow chart of the experiment test-rig is shown in the Fig. 11.

In the case of gradually increasing the load, the slewing bearing got stuck and could not be operated finally. During the experiment, interference signals were set around the periphery. After the experiment was completed, the slewing bearing was disassembled. The disassembled picture is shown in Fig. 12. In Fig. 12, the pictures are running pulley, cage, outer ring, inner ring from left to right. As can be seen from the picture, each part has suffered damage of different degrees. These failures lead to the termination of the life of the slewing bearing.

B. ANALYSIS OF RESULTS

In order to verify the effectiveness of the proposed method. RNN, LSTM and LSTM-RNN are used to compare with the method in this paper.

In these predictive models, there are four important hyperparameters which are learning rate, epoch, batch size and neurons. According to experience, the range of learning rate is from 0.001 to 0.0001. The curve of training cost should follow the law of slide-type descent. When the curve of training cost does not follow this rule, the magnitude of the learning rate adjustment can be determined based on error function of each iteration. If the error rate is reduced relative to the previous iteration, the learning rate can be increased by 5%. If the error rate increases, it means that the optimal value is skipped and the learning rate should be reduced to 50%. The learning rate should be adjusted until the curve of training cost follow the law of slide-type descent. The selection of epoch: Choose a conservative epoch based on relevant experience

TABLE 3. The optimal hyperarameter of each model.

Method	Learning rate	epoch	batch	neurons
RNN	0.0015	55	4	3
LSTM	0.001	40	4	2
LSTM-RNN	0.001	45	3	2
ST-LSTM	0.0015	20	3	2
GAN-ST-LSTM	0.0015	20	3	2

and increase the epoch until RMS of the error in prediction results falls to the stable stage. If epoch continues to increase, over-fitting will occur and the RMS will increase or there is no clear downward trend in RMS. The epoch at this time is what we need. Similarly, the optimal batch size and neurons are also selected by this way. After optimization, the optimal hyperparameters of each model are shown in Table 3.

A rolling window will be set up when training data. The rolling window contains 10 temporal indicators and 10 corresponding spatial indicators which are used as inputs. The outputs of the training set are the corresponding RUL. The inputs of the test set are also contained in anther rolling window and the inputs are the one temporal indicator and one corresponding spatial indicator behind the training set. When a set of prediction result comes out, the rolling window of the training set and test set will move forward by one unit. The process will stop when the entire process of life prediction is completed.

The prediction results of these methods are shown in Fig. 13. In these figures, the dotted lines represent the boundary of confidence interval (CI) which can be achieved by the method of bootstrap sampling. The last 600 points are used as prediction points and set the service time to 0 at the beginning of the prediction. The ordinate represents the RUL of slewing bearing. It can be seen that the prediction result of RNN is worst because it only depends on the single state of the previous training data, which causes not matching between the objective function and the predicted objective function. In addition, the prediction results of ST-LSTM and GAN-ST-LSTM are much better than those of LSTM and LSTM-RNN. At most of the time, the predicted results of LSTM are not within the 90% confidence interval and they are not stable. Moreover, compared with LSTM in the early prediction stage, the prediction accuracy of LSTM-RNN do not significantly improve. In the later prediction stage, the prediction results tend to be more stable. Compared with RNN, LSTM and LSTM-RNN, the accuracy of prediction result is significantly improved by proposed ST-LSTM. It should be noted that ST-LSTM is the first improvement of LSTM in this paper. The prediction results of ST-LSTM are all in the 90% confidence interval, and the stability is better. Because of the existence of ST gate, ST-LSTM has ST characteristics. RUL can be effectively combined with spatial and temporal indicators by the ST gate in ST-LSTM, which solves the problem of data sparsity. The GAN-ST-LSTM is the second improvement of LSTM. GAN-ST-LSTM can fine tune the prediction model

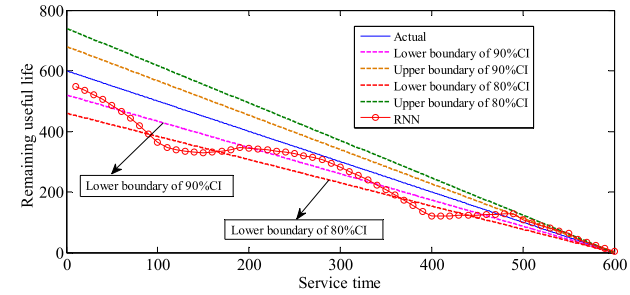

(a) The prediction result of RNN

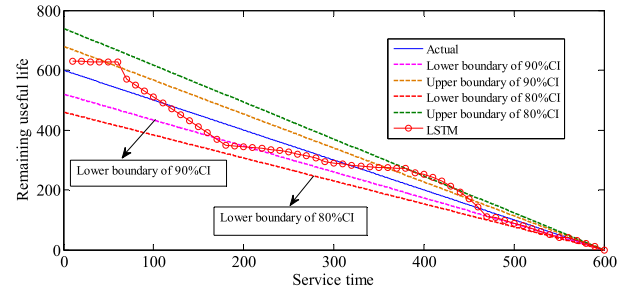

(b) The prediction result of LSTM

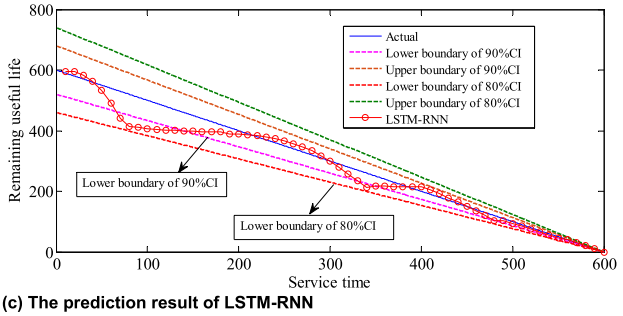

(c) The prediction result of LSTM-RNN

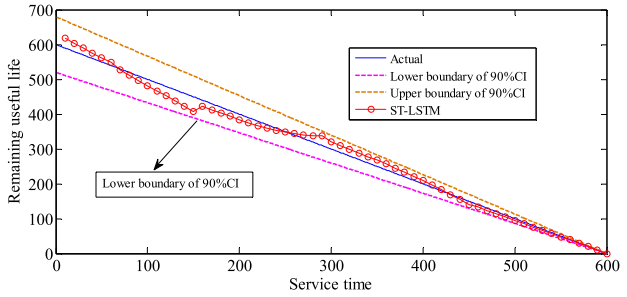

(d) The prediction result of ST-LSTM

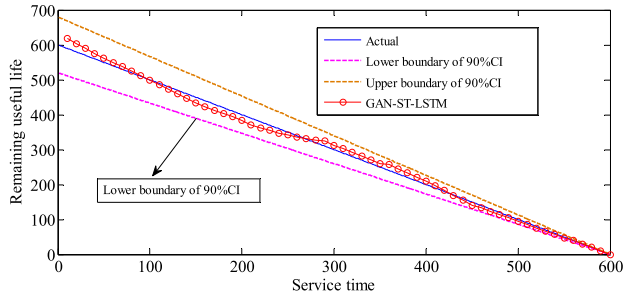

(e) The prediction result of GAN-ST-LSTM

FIGURE 13. The result of life prediction.

of ST-LSTM. The discriminator discriminates the prediction model generated by the generator ST-LSTM. If the model

TABLE 4. Prediction results of five methods.

Method	MAE	RMSE	RAPE
RNN	49.24	63.76	2.67×10^{-4}
LSTM	28.42	36.37	1.05×10^{-4}
LSTM-RNN	23.07	35.62	2.15×10^{-5}
ST-LSTM	12.51	15.57	4.13×10^{-6}
GAN-ST-LSTM	9.78	11.94	4.02×10^{-6}

is inaccurate, the prediction model generated by the generator can be re-adjusted. When the generator can't discriminate the generated model and the real model, the prediction result will be output. As seen from Fig. 13(d) and Fig. 13(e), the predicted model of GAN-ST-LSTM is adjusted faster at around 150 point and 290 point than ST-LSTM. The model accuracy of GAN-ST-LSTM is also higher than ST-LSTM.

In order to intuitively represent the performance of each predictive model, mean absolute error (MAE), root mean square error (RMSE) and mean absolute percent error (MAPE) are used to measure the quality of the prediction result. Their corresponding formulas are as follows:

$$MAE = \frac{1}{n}\sum_{i=1}^{n}|y_i - y_i'| \tag{19}$$

$$RMSE = \sqrt{\frac{1}{n}\sum_{i=1}^{n}(y_i - y_i')^2} \tag{20}$$

$$MAPE = \frac{\sum \frac{y_i - y_i'}{y_i} \times 100\%}{n} \tag{21}$$

where n represents the total number of prediction time points; y_i indicates the actually RUL of slewing bearing; y_i' denote the prediction RUL.

As given in Table 4, each kind of prediction error of ST-LSTM is greatly reduced compared to RNN, LSTM and LSTM-RNN. The corresponding error of each model shows that the ST-LSTM model proposed in this paper has great advantages in life prediction of slewing bearing. It also shows that there is a close relationship among spatial indicator and temporal indicator and the remaining life. ST gate in ST-LSTM can adjust the prediction model well and significantly improve the accuracy of the prediction. The GAN-ST-LSTM is the secondary improvement based on ST-LSTM in this paper, whose speed adjustment is accelerated within adjustable range. Moreover, the predicted results of the GAN-ST-LSTM with the slightly fine-tuned prediction mode are better than ST-LSTM.

V. CONCLUSION

High quality data and accurate mathematical model are both important in life prediction. This paper reports some creative and effective work to enhance RUL of slewing bearing. (1) A novel algorithm based on balance position is proposed to discriminate spurious fluctuations of vibration signal, which can improve the quality of sensors' data obviously. (2) The connection between spatial-temporal indicators and RUL is established by ST-LSTM to solve the data sparsity. ST-LSTM model can predict the RUL of a slewing bearing from multiple dimensions, not only time series. Compared with the typical prediction models such as RNN, LSTM, and LSTM-RNN, the relative life prediction accuracy of ST-LSTM is improved by 78.29%, 69.7% and 60.9%. Also, based on generative adversarial networks (GAN), GAN-ST-LSTM is constructed to accelerate speed of model adjustment significantly. In the future, the method proposed in this paper will be verified in more real-time monitoring platform and more accurate models will be obtained.

REFERENCES

[1] B. Zhang, H. Wang, Y. Tang, B. Pang, and X. Gao, "Residual useful life prediction for slewing bearing based on similarity under different working conditions," *Exp. Techn.*, vol. 42, no. 3, pp. 279–289, Jun. 2018.

[2] Y. Feng, X.-D. Huang, R.-J. Hong, and J. Chen, "Online residual useful life prediction of large-size slewing bearings—A data fusion method," *J. Cent. South Univ.*, vol. 24, no. 1, pp. 114–126, Jan. 2017.

[3] B. Y. Kosasih, W. Caesarendra, K. Tieu, A. Widodo, C. A. Moodie, and A. K. Tieu, "Degradation trend estimation and prognosis of large low speed slewing bearing lifetime," *Appl. Mech. Mater.*, vol. 493, pp. 343–348, Jan. 2014.

[4] J. Yu, "Bearing performance degradation assessment using locality preserving projections and Gaussian mixture models," *Mech. Syst. Signal Process.*, vol. 25, no. 7, pp. 2573–2588, Oct. 2011.

[5] P. Ding, H. Wang, W. Bao, and R. Hong, "HYGP-MSAM based model for slewing bearing residual useful life prediction," *Measurement*, vol. 141, no. 2019, pp. 162–175, Jul. 2019.

[6] X. Gao, X. Huang, H. Wang, R. Hong, and J. Chen, "Effect of raceway geometry parameters on the carrying capability and the service life of a four-point-contact slewing bearing," *J Mech Sci Technol*, vol. 24, no. 10, pp. 2083–2089, Oct. 2010.

[7] X. Yan, Y. Liu, and M. Jia, "A feature selection framework-based multiscale morphological analysis algorithm for fault diagnosis of rolling element bearing," *IEEE Access*, vol. 7, pp. 123436–123452, 2019, doi: 10.1109/access.2019.2937751.

[8] J. Deutsch and D. He, "Using deep learning-based approach to predict remaining useful life of rotating components," *IEEE Trans. Syst. Man Cybern, Syst.*, vol. 48, no. 1, pp. 11–20, Jan. 2018.

[9] A. Nait Aicha, G. Englebienne, K. Van Schooten, M. Pijnappels, and B. Kröse, "Deep learning to predict falls in older adults based on daily-life trunk accelerometry," *Sensors*, vol. 18, no. 5, p. 1654, May 2018.

[10] L. Ren, Y. Sun, H. Wang, and L. Zhang, "Prediction of bearing remaining useful life with deep convolution neural network," *IEEE Access*, vol. 6, pp. 13041–13049, 2018.

[11] Y. Qian, R. Yan, and R. X. Gao, "A multi-time scale approach to remaining useful life prediction in rolling bearing," *Mech. Syst. Signal Process.*, vol. 83, pp. 549–567, Jan. 2017.

[12] M. Yakout, A. Elkhatib, and M. G. A. Nassef, "Rolling element bearings absolute life prediction using modal analysis," *J. Mech. Sci. Technol.*, vol. 32, no. 1, pp. 91–99, Jan. 2018.

[13] B. Zhang, L. Zhang, and J. Xu, "Degradation feature selection for remaining useful life prediction of rolling element bearings," *Qual. Reliab. Eng. Int.*, vol. 32, no. 2, pp. 547–554, Mar. 2016.

[14] D.-S. Yoo, J. Lim, and M.-H. Kang, "ATSC digital television signal detection with spectral correlation density," *J. Commun. Netw.*, vol. 16, no. 6, pp. 600–612, Dec. 2014.

[15] W. Ahmad, S. A. Khan, M. M. M. Islam, and J.-M. Kim, "A reliable technique for remaining useful life estimation of rolling element bearings using dynamic regression models," *Rel. Eng. Syst. Saf.*, vol. 184, pp. 67–76, Apr. 2019.

[16] W. Ahmad, S. A. Khan, and J.-M. Kim, "A hybrid prognostics technique for rolling element bearings using adaptive predictive models," *IEEE Trans. Ind. Electron.*, vol. 65, no. 2, pp. 1577–1584, Feb. 2018.

[17] J. B. Ali, B. Chebel-Morello, L. Saidi, S. Malinowski, and F. Fnaiech, "Accurate bearing remaining useful life prediction based on Weibull distribution and artificial neural network," *Mech. Syst. Signal Process.*, vols. 56–57, pp. 150–172, May 2015.
[18] L. Eren, T. Ince, and S. Kiranyaz, "A generic intelligent bearing fault diagnosis system using compact adaptive 1D CNN classifier," *J. Signal Process. Syst.*, vol. 91, no. 2, pp. 179–189, Feb. 2019.
[19] C. Ren-Xiang, "Rolling bearing fault identification based on convolution neural network and discrete wavelet transform," *J. Vib. Eng. Technol.*, vol. 31, no. 5, pp. 883–891, May 2018.
[20] L. Guo, N. Li, F. Jia, Y. Lei, and J. Lin, "A recurrent neural network based health indicator for remaining useful life prediction of bearings," *Neurocomputing*, vol. 240, pp. 98–109, May 2017.
[21] H. Wang, M. Tang, and X. Huang, "Smart health evaluation of slewing bearing based on multiple-characteristic parameters," *J Mech Sci Technol*, vol. 28, no. 6, pp. 2089–2097, Jun. 2014.
[22] J. Zhu, N. Chen, and W. Peng, "Estimation of bearing remaining useful life based on multiscale convolutional neural network," *IEEE Trans. Ind. Electron.*, vol. 66, no. 4, pp. 3208–3216, Apr. 2019.
[23] A. Z. Hinchi and M. Tkiouat, "Rolling element bearing remaining useful life estimation based on a convolutional long-short-term memory network," *Procedia Comput. Sci.*, vol. 127, pp. 123–132, Jan. 2018.
[24] X. Wang, J. Wu, C. Liu, H. Yang, Y. Du, and W. Niu, "Exploring LSTM based recurrent neural network for failure time series prediction," *Beijing Hangkong Hangtian Daxue Xuebao/J. Beijing Univ. Aeronaut. Astronaut.*, vol. 44, no. 4, pp. 772–784, Apr. 2018.
[25] R. Wang, F. Nie, R. Hong, X. Chang, X. Yang, and W. Yu, "Fast and orthogonal locality preserving projections for dimensionality reduction," *IEEE Trans. Image Process.*, vol. 26, no. 10, pp. 5019–5030, Oct. 2017.
[26] P. Ding, H. Wang, W. Bao, and R. Hong, "HYGP-MSAM based model for slewing bearing residual useful life prediction," *Exp. Techn.*, vol. 43, no. 2019, pp. 341–358, Feb. 2019.
[27] Q. Yu, R. Wang, B. N. Li, X. Yang, and M. Yao, "Robust locality preserving projections with cosine-based dissimilarity for linear dimensionality reduction," *IEEE Access*, vol. 5, pp. 2676–2684, 2017.
[28] M. Wielgosz, A. Skoczeń, and M. Mertik, "Using LSTM recurrent neural networks for monitoring the LHC superconducting magnets," *Nucl. Instrum. Methods Phys. Res. A, Accel. Spectrom. Detect. Assoc. Equip.*, vol. 867, pp. 40–50, Sep. 2017.
[29] F. Karim, S. Majumdar, H. Darabi, and S. Chen, "LSTM fully convolutional networks for time series classification," *IEEE Access*, vol. 6, pp. 1662–1669, 2018.
[30] G. M. Wang, "A generative adversarial network based on energy function," *Zidonghua Xuebao/Acta Automatica Sinica*, vol. 44, no. 5, pp. 793–803, May 2018.
[31] W. Tang, S. Tan, B. Li, and J. Huang, "Automatic steganographic distortion learning using a generative adversarial network," *IEEE Signal Process. Lett.*, vol. 24, no. 10, pp. 1547–1551, Oct. 2017.
[32] X. Yi and P. Babyn, "Sharpness-aware low-dose CT denoising using conditional generative adversarial network," *J. Digit. Imag.*, vol. 31, no. 5, pp. 655–669, Oct. 2018.
[33] B. Huang, W. Chen, X. Wu, C.-L. Lin, and P. N. Suganthan, "High-quality face image generated with conditional boundary equilibrium generative adversarial networks," *Pattern Recognit. Lett.*, vol. 111, pp. 72–79, Aug. 2018.
[34] Z. Wang, Z. Chen, and F. Wu, "Thermal to visible facial image translation using generative adversarial networks," *IEEE Signal Process. Lett.*, vol. 25, no. 8, pp. 1161–1165, Aug. 2018.

WEIGANG BAO is currently pursuing the M.S. degree in mechanical engineering with Nanjing Tech University. His current research interests include condition monitoring, signal processing, fault diagnosis, and the algorithm of artificial intelligence.

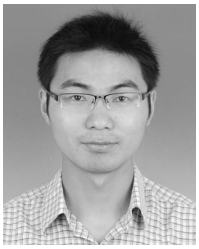

XIAODONG MIAO received the B.S. and Ph.D. degrees in mechanical engineering from the Nanjing University of Aeronautics and Astronautics, Nanjing, China, in 2008 and 2013, respectively. He is currently an Assistant Professor of mechanical engineering with Nanjing Tech University. His research interests include sensors and signal processing, machinery condition monitoring, fault diagnostics, and applications of artificial intelligence.

HUA WANG received the B.S. and Ph.D. degrees in mechanical engineering from Harbin Engineering University, Harbin, China, in 2001 and 2006, respectively. He has been holding a Short-Term Visiting position at the Dublin Institute of Technology, Ireland, since 2010. He was a Visiting Scholar with the Department of Mechanical and Industrial Engineering, University of Massachusetts, USA, from 2014 to 2015. He is currently a Full Professor of mechanical engineering with Nanjing Tech University. His research interests include machinery condition monitoring and fault diagnosis, mechanical signal processing, intelligent fault diagnostics, and remaining useful life prediction. He is also the Senior Member of the China Mechanical Engineering Society. He is also a Reviewer for several SCI-indexed journals in this field.

GUICHAO YANG, photograph and biography not available at the time of publication.

HAO ZHANG, photograph and biography not available at the time of publication.